Aperito Online Publishing

Journal of Mechanical and Automation Engineering

Received: Nov 17, 2015
Accepted: Dec 01, 2015
Published: Dec 04, 2015

http://dx.doi.org/10.14437/JMAE-1-102 Research Li-Hong Juang, J Mech Auto Eng 2015, 1:1

Levitation Effect Study based on a Disc-type Piezoelectric Ultrasonic Stator

Li-Hong Juang* **and Lixin Zheng**

Science & Technology Innovation Center, Engineering College, HuaQiao University, Fujian, P.R. China

Abstract

The objective of the paper is to gain a deeper understanding of the levitating behavior of the disc type ultrasonic stator for possible application on moving object. For the purpose, some axial vibration measurements were made to investigate levitation motion on the stator surface and explore its possible application on the linear, surfing and shaft types of bearing less ultrasonic motor. Dynamic response also was investigated and compared with some analytical results. The result showed that the levitation capacity decreased with driving frequency increase.

Keywords: Levitation motion; Surfing; Bearing less

***Corresponding Author:** Li-Hong Juang, Science & Technology Innovation Center, Engineering College, HuaQiao University, Fujian, P.R. China; E-mail: puuan.juang@msa.hinet.net

Introduction

Piezoelectric ultrasonic stators have been routinely used as driving sources of ultrasonic motors. Their driving characteristics result from the frictional contact force between the stator and rotor. However, in addition to rotating a stator by contact friction, piezoelectric ultrasonic stators can also levitate and transport objects [1] by non-contact ultrasonic radiation. Hashimota and co-workers [2, 3] have proven that a 10-kg planar object can be levitated without a reflector. Hatano et al. [9] have reported that small objects of a few grams were levitated on the nodal points by the excitation of a standing acoustic field. Moroney et al. [4] have proposed levitating and transporting small objects using 4MHz ultrasonic driving frequency.

As known, the use of a contact bearing will reduce the performance of the ultrasonic motor due to friction loss. Through ultrasonic levitation, a stator can be made into a non-contact bearing-less structure with linear or planar motion [5]. So, the efficiency of the ultrasonic motor can also be raised. Since the linear ultrasonic motor has few moving parts and is lightweight and bearing-less, it is ideal for space applications where problems of bearing seizure, reliability and weight are key concerns [6]. Newton et al. [7] have developed a type of linear hybrid transducer piezoelectric motor. The motor consists of a longitudinal actuator, which provides output displacement and force, and two alternating clamping actuators, which provide the holding force. This motor has the advantages of being lightweight, and having macro- and micro-positioning, large force/velocity output and less contact.

This new variation of the linear motor has numerous other applications. The Kurosawa linear motors [4] that incorporate piezoelectric stacks can be driven with sinusoidal voltages at high frequencies to achieve a reported maximum speed of 50mm/sec and a maximum force output of 0.5kgf. The force outputs of both these designs are limited by the inability of a piezoceramic to withstand shears forces due to less contact. The Burleigh linear motor has been proposed [8], which can operates well as a micro-positioner with a maximum speed of 2mm/sec and a maximum force output of 1.5kgf. Speed improvements are realized by the ability to drive lower voltage at higher frequencies. Helin et al. [9] have presented theory, simulation results and experimental study of a slider displacement at a nanometer scale in a linear ultrasonic motor using Lamb and Rayleigh waves. They made the first attempt to describe the energy transfer from the acoustic wave to a slider. Their analysis model has shown that the mechanism is sequential with alternative phases of levitation and contact with step-like behavior of the slider velocity. Kurosawa et al. [10] have demonstrated the first success of a linear ultrasonic motor with 10MHz Rayleigh waves. The slider moved in the opposite direction of the propagation through a frictional drive. Helin et al. [11] fabricated several linear ultrasonic motors using Lamb and Rayleigh waves with the highest frequencies. The positioning of a levitated object can be accurate by means of time-controlled electrical excitation. A detailed description can be found in a reference [12] of an inter-digital transducer for Rayleigh wave excitation and Lamb waves. The propagation of these surfaces

http://dx.doi.org/10.14437/JMAE-1-102

acoustic waves generates a retrograde elliptic motion of surface particles [12]. By contacting a slider onto the substrate surface, it is pulled by the surface particles through friction force in the opposite direction of the wave propagation. Kurosawa et al. [14] have proposed an X-Y linear motor that operates at 10MHz in two dimensions and uses a $LiNbO_3$ wafer of three inches in diameter. Kurosawa et al. [15] have demonstrated the operation of an HF band (3-30MHz) ultrasonic motor at 20MHz, which was made possible by operating the Rayleigh wave; a type of surface acoustic wave was applied to the linear ultrasonic motors. Takahashi et al. [16] have experimentally investigated the operation conditions and basic performance of linear ultrasonic motors under high-frequency operation. The most significant result of this research was the discovery of the high output force density of the friction drive. The output force density is 50N/mm^2. However, the actual output force was 1 mN because the tested slider was one steel ball. The maximum speed and maximum acceleration were 0.8m/s and 900m/s^2. Kurosawa and Ueha [17] and Kuribayashi and Ueha [18] have succeeded in the circulation of the power flow in a vibration system of a travelling wave type linear motor having two longitudinal vibrators and a flexural vibrating bar for a wave guider using an electric circuit.

The objective of the paper is to gain a deeper understanding of the levitating behavior of the disc type ultrasonic stator for possible application on moving object. On the surface of a piezoelectric ultrasonic stator, where an object is levitated and moved by the ultrasonic field radiated from the stator into the air gap between the levitated object and the stator. Although in this research we develop a disc-type ultrasonic stator mainly based on lateral elliptic motion, we find some levitation effect when the stator is driven at driving frequency. Most ultrasonic motors inherit some special properties such as high output torque, quick response, and large holding torque without energy dissipation and free magnetic field operation. They result from the use of piezoelectric ceramic, ultrasonic vibration and the friction force between the stator and the rotor. However, they also restrict the applied range of the motor. So by studying levitation effect, we search the possibility to make the non-contact bearing-less structure of the stator to be explored the levitating behavior and developed into another application like ultrasonic bearing and transportation system. In this research, according to stress wave propagation theory, levitation characteristics including levitation displacement, velocity and force formulary are derived and checked by experimental measurement.

Levitation Characteristics

Figure 1 shows that a planar object can be levitated by a normally radiated acoustic wave when the stator is excited at resonant frequency or in harmonic excitation. For exploring the surface levitation characteristic of the stator, the levitated object must be rigid body. So it can avoid consuming some energy from the stator. Meanwhile, the dimension of the levitated object, especially on the button surface is larger than the ultrasonic wavelength.

Figure 1: Configuration of the stator.

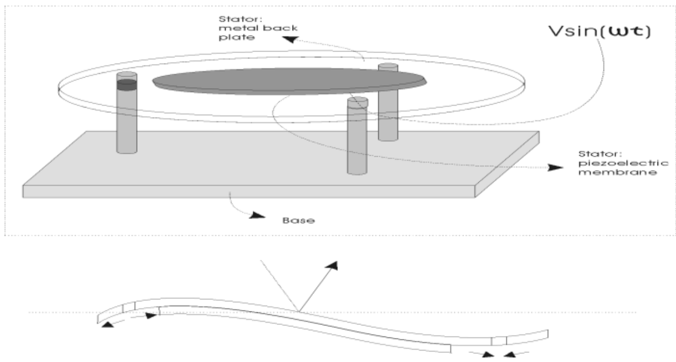

Levitation Displacement

The levitation displacement of the stator surface is induced by flexural vibration caused from shear force and bending interaction between piezoelectric membrane and metal back plate, as shown in Figure 2.

Figure 2: Schematic diagram of ultrasonic levitation [8].

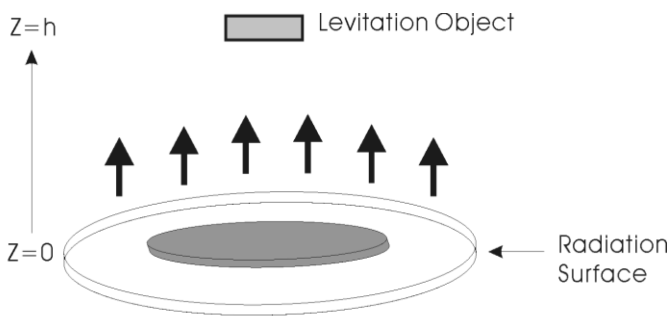

To derive the levitation displacement, the governing equation of an elastic circular membrane in terms of polar coordinates based on an elastic circular plate due to lateral elliptic motion needs to be involved again as follows

$$\nabla^4 w(r,\theta,t) = \frac{\partial^2 w(r,\theta,t)}{c_0^2 \partial t^2}, \qquad (1)$$

Where c_0 is the phase velocity of wave. Assuming the solution has a form as

$$w(r,\theta,t) = R(r)\Theta(\theta)(A\cos\omega + B\sin\omega t), \qquad (2)$$

Using variable separation method leads to

$$\frac{R''}{R} + \frac{1}{r}\frac{R'}{R} + \beta^2 = -\frac{\Theta''}{\Theta} = \gamma^2, \beta^2 = \omega^2 / c_0^2 \qquad (3)$$

The solution for R and   are as follows

$$\Theta = A_1 \cos\gamma\theta + A_2 \sin\gamma\theta \qquad (4)$$

$$R = B_1 J_n(\beta r) + B_2 Y_n(\beta r) \qquad (5)$$

Where J_n and Y_n are the Bessel function of first and second kind. Additionally, $w(r,\theta,t) = w(r,\theta + 2\pi, t)$ periodicity condition needs to be satisfied. When $r = 0$, $Y_n \to \infty$, so $B_2 = 0$. Then according to the boundary condition as follows

$$w(a,\theta,t) = 0, \theta = 0^\circ, 90^\circ, 210^\circ \to R(a) = 0 \qquad (6)$$

Substituting (6) into (5) gets the resonant frequency equation

$$J_n(\beta a) = 0 \qquad (7)$$

By non-trivial solution, the resonant frequency can be express $\omega_{nm} = \beta_{nm} c_0$ (8)

Where n and m are the mode numbers. Finally, the levitation displacement can be expressed a Fourier series summation as

$$w(r,\theta,t) = \sum_{m=1}^{\infty} \left\{ \begin{array}{l} \sum_{n=0}^{\infty} W_{nm}(A_{nm}\cos\omega_{nm}t + B_{nm}\sin\omega_{nm}t) \\ + \sum_{n=1}^{\infty} \tilde{W}_{nm}(\tilde{A}_{nm}\cos\omega_{nm}t + \tilde{B}_{nm}\sin\omega_{nm}t) \end{array} \right\} \qquad (9)$$

The substitutive variables W_{nm} and $\tilde{W}_{nm}$ are given by

$$W_{nm} = J_n(\beta_{nm} r)\cos n\theta, \tilde{W}_{nm} = J_n(\beta_{nm} r)\sin n\theta \qquad (10)$$

They are defined as normal modes and have 90° difference each other. Figure 3(a)-(c) shows the vibration amplitude distribution of the stator in the spatial Fourier spectrum for 75, 83 and 98 kHz.

Figure 3: The vibration amplitude distribution of the stator in the spatial Fourier spectrum for (a) 75kHz, (b) 83kHz and (c) 98kHz.

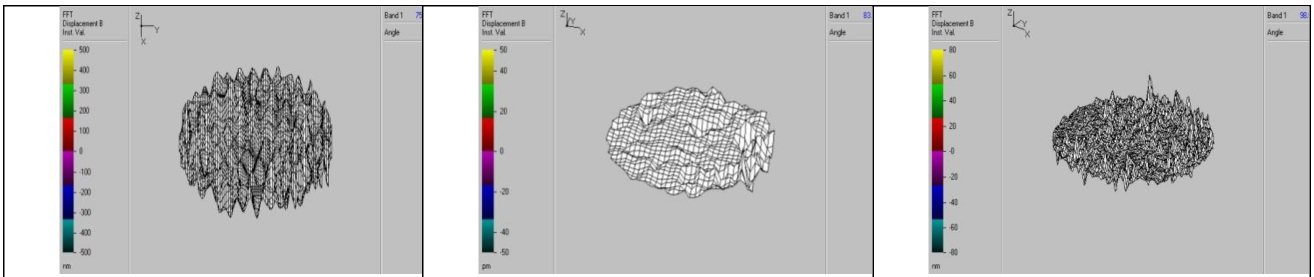

(a) (b) (c)

Levitation Frequency

The levitation frequencies are equal to resonant frequencies. From (8), we can acquire it as follows

$$f_l = \frac{\beta_{nm} c_0}{2\pi} \tag{11}$$

The reference [18] lists some relative value for finding β_{nm}. However our interesting frequency rang is ultrasonic frequency. We mainly explore the levitation effect at the driving frequency of the stator.

Levitation Velocity

Figure 4 shows the movement velocity and direction of levitated object under the flexural vibration mode. Because the ultrasonic wave does not propagate normal to the stator, the radial and tangential velocity components need to be considered.

Figure 4: The movement velocity and direction of levitated object under the flexural vibration mode.

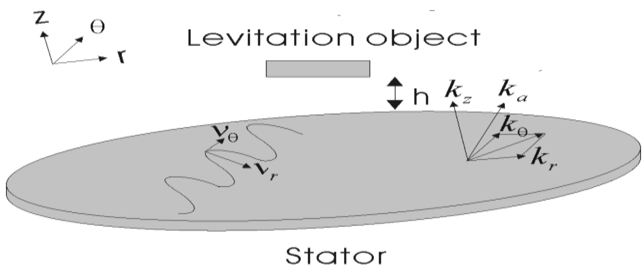

For this, first the radial and tangential displacements need to be derived. According to Kirchoff assumption, r and θ direction displacements based on z direction displacement are given by

$$u_r = u - \frac{\partial w}{\partial r}$$
$$u_\theta = v - \frac{\partial w}{\partial \theta} \tag{12}$$

Where u and v are mid-plane displacement in $\vec{e}_r$ and $\vec{e}_\theta$. The resulting displacement will be

$$u_r = \left\{ f' + (n/r) h_z + k_a h_r \right\} \cos n\theta e^{-j\omega_{nm} t} \tag{13}$$

$$u_\theta = \left\{ -(n/r) f + k_a h_r - h_z' \right\} \sin n\theta e^{-j\omega_{nm} t} \tag{14}$$

The substitutive variables f, h_r and h_z are given by

$$f(r) = AJ_n(\alpha_{nm} r)$$
$$h_r(r) = B_1 J_{n-1}(\beta_{nm} r) + B_2 J_{n+1}(\beta_{nm} r) \tag{15}$$
$$h_z(r) = B_3 J_n(\beta_{nm} r)$$

Where $k_a = \sqrt{k_r^2 + k_\theta^2}, k_r = \frac{\omega_{nm}}{\vartheta_r}, k_\theta = \frac{\omega_{nm}}{\vartheta_\theta}, \vartheta_r = \sqrt{\frac{E_r}{\rho}},, \vartheta_\theta = \sqrt{\frac{E_\theta}{\rho}}, \alpha_{nm} = \sqrt{\beta_{nm}^2 - k^2}$ are wave number and sound speeds in radial and tangential vibration. So the relative velocity can be obtained by differentiating (9), (13) and (14). They are as follows

$$v_z = -j\omega_{nm} w \tag{16}$$

$$v_r = -j\omega_{nm} u_r \tag{17}$$

$$v_\theta = -j\omega_{nm} u_\theta \tag{18}$$

http://dx.doi.org/10.14437/JMAE-1-102

As Figure 5 shows that the levitated object will be transported by a traveling wave propagating on the stator. Figure 6(a)-(c) shows the vibration velocity distribution of the stator in the spatial pattern for 75, 83 and 98 kHz

Figure 5: Explanation of travelling wave motion on a stator [8].

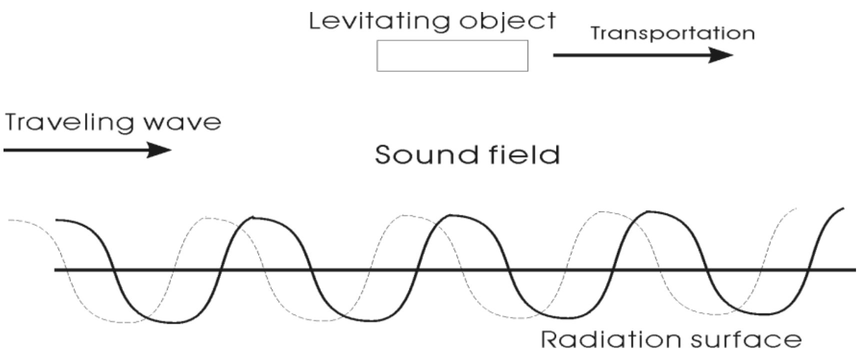

Figure 6: The vibration velocity distribution of the stator in the spatial pattern for 75 kHz, 83 kHz and 98 kHz.

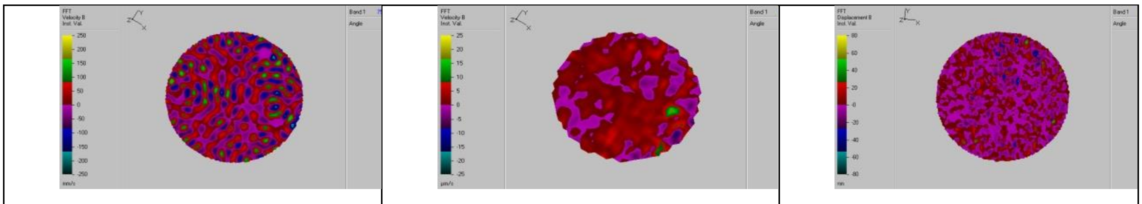

(a)	(b)	(c)

Levitation Force

The levitation force is induced from the surface stress resulted from flexure strain. From the stress-displacement equation

$$\tau_z = \mu\left(\frac{\partial w}{r\partial\theta} + \frac{\partial w}{\partial r}\right) \quad (19)$$

Substituting (9) into (19), the stress equation can be obtained

$$\tau_z = \mu J_0(k_a r)\left\{2B'\beta_{nm}\cosh\beta_{nm}r - 2Bk_a\sinh\beta_{nm}r - A\frac{k_a^2+\beta_{nm}^2}{\alpha_{nm}^2-\beta_{nm}^2}\cosh\alpha_{nm}r\right\}e^{-j\omega_{nm}t} \quad (20)$$

The model of [32] is used to calculate the levitation force, which is a summation of each stress component and expressed as

$$\prod = \iint \tau_z dr d\theta - P \quad (21)$$

Where P is the loading weight of the levitation object. In the following section, detailed laser probe measurements of the actual displacement on the stator to analyze the nature of levitation at driving frequencies are reported.

Simulation and Test

The measurements of actual displacement on the stator were performed using the laser heterodyne technique. Three major resonances of interest in ultrasonic levitation are designated as 75kHz, 83kHz and 98kHz. The frequencies of these resonances were independent of the stator thickness, but were related to the lateral periodicity of the stator. As the wavelength of the transverse waves becomes comparable with the time of the circumferential distance between two fixed points, ultrasonic displacement on the stator is expected to be more non-uniform, as shown in Figure 3(a)-(c). The plot in Figure 7 (a)-(c) shows the complex vibration pattern at 75, 83 and 98kHz corresponding to three different circumferential locations(120°-90°-150°). Their patterns are not similar to each other due to non-symmetry boundary. In addition, the results reveals that when the circumferential spacing is the time of shear wavelength, a standing wave pattern will be created.

http://dx.doi.org/10.14437/JMAE-1-102

Figure 7: Variation of the vibration velocity at (a) 75kHz, (b) 83.81kHz and (c) 98kHz corresponding to three different circumferential locations(here a.u., a=around, u=unit, means taking circumference as normal unit).

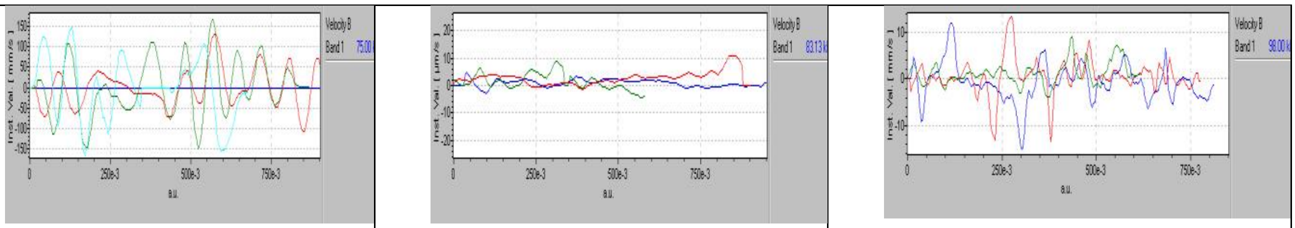

(a) (b) (c)

The plot in Figure 8 (a)-(c) shows the complex vibration pattern at 75, 83 and 98kHz corresponding to any two different diameter locations. The different patterns are expected due to non-equal included fixed points. From laser scan's pattern, we can observe small amplitude variations at 83 and 98kHz. This is probably because of the reduced attenuation at higher driving frequency. This uniform ultrasonic displacement observed on the surface of the stator at 75kHz. It is a clear indication of efficient coupling of the mechanical energy piezoelectric membrane to the metal back plate. For a z-polarized traveling wave incident on the stator, Bragg scattering could occur, especially at higher resonant frequency. Meanwhile, a spatial modulation of the phase fronts is produced by the properties of the non-symmetry boundary. The stator is excited at 75, 83 and 98kHz. The levitated object is hanged with springs at plane and vertical direction. Initially, it is placed at the center of the stator. The movement amplitude and the levitation distance are measured with three separate gauge meters. The levitated object $3\times3\times3mm^3$ of size and 0.01g of weight. Figure 9 shows an example of measured levitation distance as a function of weight at three different driving frequencies. The result shows that the levitation capacity decreases with driving frequency increase.

Figure 8: Variation of the vibration velocity at (a) 75kHz, (b) 83.81kHz and (c) 98kHz corresponding to two different circumferential locations(here a.u., a=around, u=unit, means taking circumference as normal unit)

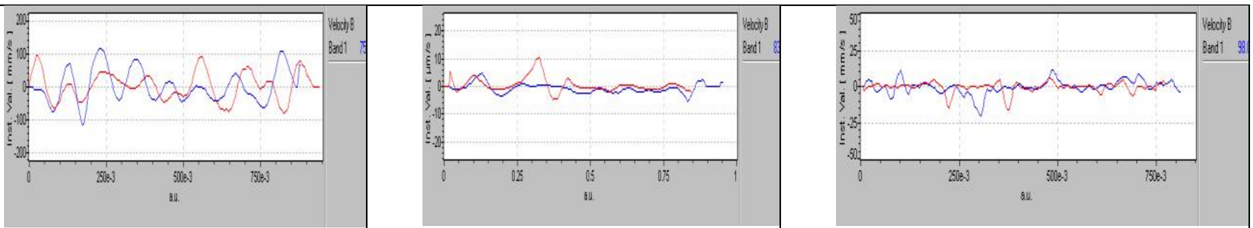

(a) (b) (c)

Figure 9: The example of measured levitation distance as a function of weight at three different driving frequencies.

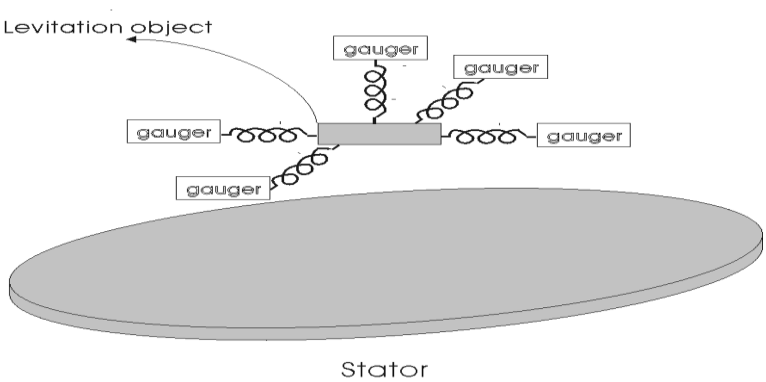

Summary

In this research, vibration displacement and velocity efficiency were measured in axial vibration measurement. The results showed that the vibration patterns were non-uniform with Bragg scattering. From axial vibration measurement, the sensitivity values were also obtained. Meanwhile axial vibration measurement was made to investigate levitation motion on the stator surface. An axial vibration levitation motion can be applied to linear, surfing and shaft types of bearingless ultrasonic motor. Dynamic response was investigated and compared with several analytical results mentioned above.

Acknowledgement

The authors deeply acknowledge the financial support from HuaQiao University, Fujian, P.R. China under the HuaQiao Scientific Research Foundation for Talents plan.

References

1. Yamayoshi, Y.; Hirose, S. Ultrasonic motor not using mechanical friction force. *International Journal of Applied Electromagnetic Materials* 3 (1992), pp. 179-182.
2. Hashimoto, Y.; Koike, Y.; Ueha, S. Near field acoustic levitation using flexural vibration mode. *Ultrasonics World Congress Proceedings*. Berlin, 1995, pp. 835-837.
3. Hashimoto, Y.; Koike, Y.; Ueha, S. Near-field acoustic levitation of planar specimens using flexural vibration. *Journal of the Acoustic Society of Japan* 100 (1996), pp. 2057-2060.
4. Ueha, S.; Hashimoto, Y.; Koike, Y. Non-contact transportation using near-field acoustic levitation. *Ultrasonics* 38 (2000), pp. 26-32.
5. Hatano, H.; Kanai, Y.; Ikegami, Y.; Fujii, T.; Saito, K. Ultrasonic levitation and positioning of sample. *Japanese Journal Applied Physics* 21 (Supplement 3) (1982), pp. 202-206.
6. Moroney, M.; White, R. M.; Howe, R. T. Ultrasonic micromotors. *IEEE Ultrasonics Symposium*. Montreal, 1989, pp. 745-747.
7. Kurosawa, M.; Yamada, H.; Ueha, S. Hybrid transducer type ultrasonic linear motor. *Japanese Journal Applied Physics* 28 (Supplement 28-1) (1988), pp. 156-160.
8. Burleigh Instruments Incorporation. Piezoelectric electromechanical translation apparatus. *US Patent* 3902084, 1975.
9. Helin, P.; Sadaune, V.; Druon, C.; Tritsch, J. B. linear ultrasonic motors using surface acoustic waves mechanical model for energy transfer. *International Conference on Solid-State Sensors and Actuators.* Chicago, 1997, pp. 1047-1050.
10. Kurosawa, M.; Takahashi, M.; Higuchi, T. Ultrasonic linear motor using surface acoustic waves. *IEEE Transaction on Ultrasonics, Ferroelectrics and Frequency Control* 43 (1996), pp. 901-906.
11. Helin, P.; Druon, C.; Sadaune, V. A microconveyer using surface acoustic waves in the HF band. *Proceedings of IEEE Mechatronics Symposium.* Paderburg, 1996, pp. 580-5825.
12. Viktorov, I. Rayleigh and Lamb waves. Plenum Press, 1967.
13. Kurosawa, M.; Takahashi, M.; Higuchi, T. Ultrasonic X-Y stage using 10MHz surface acoustic waves. *Proceedings of IEEE Ultrasonics Symposium.* Cannes, 1994, pp. 534-538.
14. Kurosawa, M.; Takahashi, M.; Higuchi, T. Operation condition and output force of surface acoustic wave motor. *Technical Report Institute of Electronics, Information and Communication Engineers of Japan* US97-76 (1996), pp. 43-50.
15. Kurosawa, M.; Takahashi, M.; Higuchi, T. A surface acoustic wave motor using V-shape groove guide. *Transaction on Institute of Electronics, Information and Communication Engineers of Japan* J80-A (1997), pp. 1711-1717.
16. Kuribayashi, M.; Ueha, S. Study of ultrasonic linear motor IV—electrical method of energy back flow. *Proceedings of Annual Meeting of Acoustic Society of Japan*. Japan, 1985, pp. 585-586.
17. Kurosawa, M.; Ueha, S.; Mori, E. Excitation conditions of flexural traveling waves for reversible linear motor. *Journal of the Acoustic Society of Japan* 77 (1985), pp. 1431-1439.
18. Iula, A.; Carotenuto, R.; Lamberti, N.; Pappalardo, M. A matrix model of the axle vibration of a piezoelectric motor. In *Ultrasonics* 38 (2000), pp. 41-45.